CHAPTER 3: DEVELOPMENT OF THE METHODOLOGY TO STUDY PURIFIED AND RECONSTITUTED HEMICHANNELS BY LUMINESCENCE RESONANCE ENERGY TRANSFER

INTRODUCTION

As mentioned at the end of the previous chapter, in Chapter 3 I describe some improvements in the Cx43 purification methodology and additional characterization of the preparation as well as the methodology for the generation and characterization of hemichannels of controlled subunit composition. The goals of the studies in this chapter were to develop a stable, functional preparation of purified hemichannels in which I can control the number and position of the donor and the acceptor for the LRET experiments presented in the subsequent chapters.

The methodology to produce highly-purified Cx43 hemichannels has been published by our laboratory (Bao *et al.*, 2004b), and here I just present the use of a different detergent to obtain a more stable and fully-functional preparation (see **METHODS**).

Recently, luminescence or lanthanide-based resonance energy transfer (LRET) has been used to assess inter-subunit and intra-molecular distances (Cha and Bezanilla, 1998; Vázquez-Ibar *et al*., 2002; Knauf and Pal, 2004; Posson *et al*., 2005). It has many advantages in comparison to FRET, which translate in very low background, high signal-to-noise ratio, and independence of the labeling stoichiometry, enabling LRET to measure distances in the 25-100 Å range with little uncertainty due to orientation factors (see Fig. 3.1 and Fig. 3.2). Here, I present the basic characterization of the use of the methodology in purified and reconstituted hemichannels. A significant portion of this work has been recently published (Bao *et al*., 2007).

In FRET (top panel), when acceptor and donor are in close proximity, energy is transferred from the excited donor to the acceptor. The consequences are reduced donor emission, increase acceptor emission and decrease in the lifetime of the donor excited state (FRET introduces a parallel relaxation pathway). In LRET (bottom panel), with measurements performed in a gated mode (emission recorded after μs delays following a short (ns) excitation pulse, the sensitized emission (emission of the acceptor with ms lifetime) represents the lifetime of the donors that participate in energy transfer. The stoichiometry of labeling is therefore irrelevant. Some of the advantages of LRET are listed in Fig. 3.2.

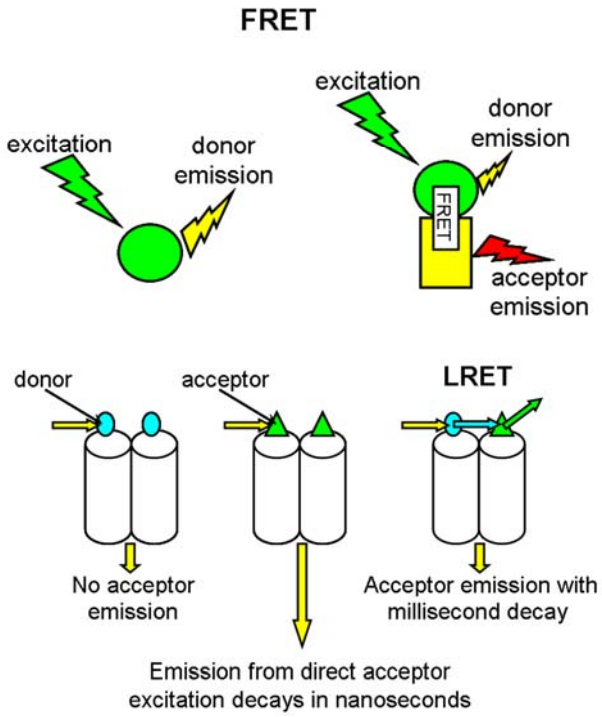

Figure 3.1: Schematic representation of FRET and LRET.

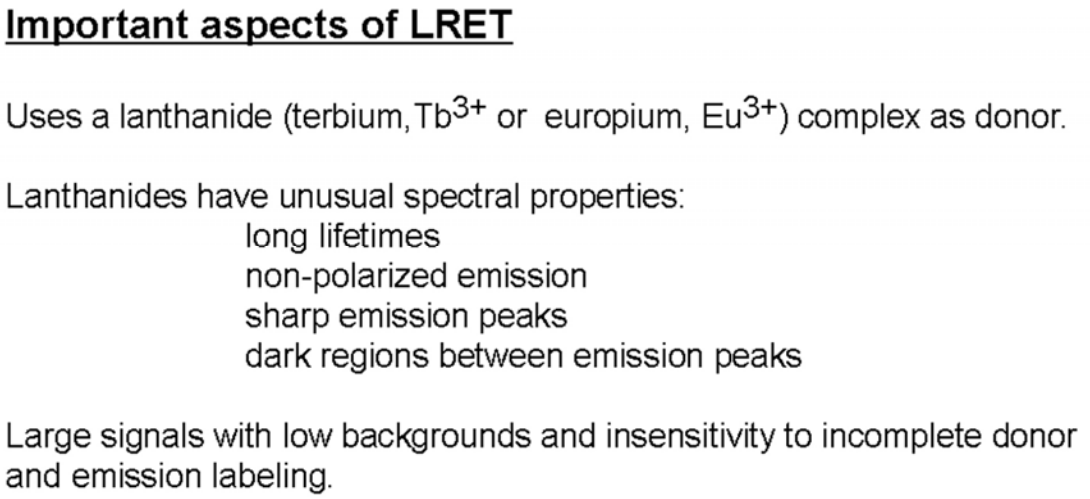

Figure 3.2: Important aspects of LRET.

MATERIALS AND METHODS

Materials

The Bac-to-Bac baculovirus expression system to generate recombinant baculovirus for Cx43 expression was purchased from Invitrogen (Carlsbad, CA). Phosphatidyl choline and phosphatidyl serine were from Avanti (Alabaster, AL). The detergents for membrane-protein extraction were obtained from Anatrace (Maumee, OH). SF900II SFM and Express Five medium was from Invitrogen (Carlsbad, CA), the Ni-NTA column from Qiagen (Valencia, CA), Biobeads SM-2 from Bio-Rad (Hercules, CA), dialysis membrane from Spectra/Pro (Rancho Dominguez, CA) and radioactive sucrose from ARC (St Louis, MO). All other chemicals were from Sigma (St. Louis, MO) `or Fisher Scientific (Houston, TX). L-α-phosphatidylcholine and L-α-phosphatidylserine were purchased from Avanti Polar Lipids (Alabaster, AL).

Insect cell culture

For the generation of baculovirus, Sf-9 cells were grown at 27 °C in SF900II SFM medium. Cells were cultured at a density of 0.5×10^6 cells/ml. For protein overexpression, High-Five insect cells were grown in suspension, in 300-ml baffled flasks containing 100 ml of Express Five medium supplemented with 2 mM glutamine. Cells (1×10^6 cells/ml) grown at room temperature were shaken at 125 rpm, and infected at a multiplicity of infection of 10.

Generation of baculovirus

Recombinant baculovirus stocks were prepared as described (Bao *et al*., 2004b; Bao *et al*., 2007). Briefly, surface-attached Sf-9 cells were transfected with recombinant bacmid DNA, and after 5 h the transfection mixture was removed and incubation proceeded in SF-900II medium at 27 °C for 72 h. After that time, viruses were harvested from the medium and used to produce a high-titer stock used for infection of cells.

Engineering plasmids coding for the single-Cys mutants

To generate the mutant plasmids used to produce recombinant baculoviruses, I employed Cys-less Cx43D2 as template. The Cys-less DNA in a plasmid to produce cRNA for oocyte injection (Bao *et al*., 2004c) was cut and ligated into pFast-Bac, which we routinely used as transfer plasmid. The I156C, I157C, S158C, F161C, K162C, V164C, V167C single-Cys mutants were produced by site-directed mutagenesis, as described in previous chapters. The 5'-phosphorylated mutagenic primers were: 5'-GCTTGCTGAGAACCTACTGCATCAGCATCCTCTTCAAG-3' (I156C); 5'-GCTTGCTGAGAACCTACTGCATCAGCATCCTCTTCAAG-3' (I157C); 5'-GCTGAGAACCTACATCATCTGCATCCTCTTCAAGTCTGTC-3' (S158C); 5'-CCTACATCATCAGCATCCTCTGCAAGTCTGTCTTCGAGGTGGCC-3' (F161C); CCTACATCATCAGCATCCTCTTCTGCTCTGTCTTCGAGGTGGCCTTCC-3' (K162C); 5'-CAGCATCCTCTTCAAGTCTTGCTTCGAGGTGGCCTTCCTGC-3' (V164C); 5'-CCTCTTCAAGTCTGTCTTCGAGTGCGCCTTCCTGCTCATCCAGTGG-3' (V167C).

DNA sequencing of all constructs was performed at the Protein Chemistry Core Laboratory of the University of Texas Medical Branch.

Expression and purification of wild-type and Cx43 mutants

Details on the expression in High-Five insect cells have been described (Bao *et al*., 2004b). In the studies presented in this chapter, I used Cx43 and Cx43-EGFP (Bao *et al*., 2004b), as well as Cys-less Cx43 and the single-Cys mutants F161C and I156C (see below). Cx43-EGFP has an enhanced green fluorescent protein (EGFP) fused to the Cx43 C-terminal end, and all the proteins have a 6 His affinity tag at the C-terminal end. Protein purification was performed essentially as described (Bao *et al*., 2004b), based on the affinity of a 6-His C-terminal tag for Ni^{2+}, but membrane solubilization and purification were carried out in decylmaltoside instead of n-octyl-β-D-glucopyranoside (octylglucoside). Briefly, High-five cells grown in suspension were infected with a recombinant baculovirus and collected by centrifugation 72 h after infection. The cells were washed and the pellets were frozen in liquid nitrogen. Frozen pellets were used for purification immediately or stored at -80°C for subsequent use. For purification, the cell pellets were thawed in a buffer containing 1 mM bicarbonate and 1 mM PMSF, and lysed with a dounce homogenizer. After addition of NaOH to 20 mM, the lysate was sonicated with a probe sonicator. After incubation on ice for 30 min, the lysate was centrifuged at 35,000 g for 30 min at 4 °C to collect the alkali-extracted membranes. Membranes were solubilized with 1% decylmaltoside in 2 M NaCl, 10 mM EDTA, 10 mM DTT, 10 mM PMSF, and 10 mM glycine/NaOH, pH 10, at a protein concentration <2 mg/ml. During purification and subsequent steps, decylmaltoside concentration was 0.3%. The solubilized suspension was sonicated and then incubated for 2 h at 4 °C with gentle rotation. Unsolubilized material was separated by ultracentrifugation at 100,000 g for 40 min at 4 °C. The solubilized protein was diluted with 15 volumes of 10 mM β-mercaptoethanol, 1 mM PMSF, 100 mM HEPES and 0.3% DM, pH 8.0. The samples were loaded onto a Ni-NTA column pre-equilibrated with the dilution buffer, at 0.5

ml/min, at 4 °C. Bound proteins were washed first with washing buffer (10 mM HEPES, pH 7.4, 10 mM KCl and 0.1 mM EDTA with 20 mM imidazole) also containing 0.3% DM. Elution was elicited with 250 mM imidazole in washing buffer.

Dephosphorylation and PKC-mediated phosphorylation of purified connexins

For dephosphorylation and PKC-mediated phosphorylation, we first treated purified Cx43 solubilized in decylmaltoside with immobilized alkaline phosphatase to remove phosphates from residues phosphorylated in the insect cells (Bao *et al*., 2004b). Then, we phosphorylated a fraction of the dephosphorylated connexins with PKC, using conditions that result in phosphorylation of all of the Ser-368 residues (1 mol of Ser-368 phosphorylated *per* mol of Cx43) (Bao *et al*., 2007).

Reconstitution of purified hemichannels in liposomes

L-α-phosphatidylcholine (PC) and L-α-phosphatidylserine (PS) were mixed at a molar ratio of 2:1. Lipids from chloroform stocks were mixed and lyophilized overnight under Argon. The dry film was rehydrated in washing buffer containing 80 mM octylglucoside, and warmed to 37 °C until it became transparent. Proteins were added to the lipid-detergent mixture and dialyzed for 24 h at room temperature (6,000-8,000-molecular-weight-cutoff dialysis membrane) against 500 ml of detergent-free washing buffer containing 10 ml of a 50% (w/v) suspension of Biobeads SM-2. After dialysis, large unilamellar vesicles of 100-nm diameter were obtained by extrusion (Mini-Extruder, Avanti). The size of the liposomes and proteoliposomes was confirmed by dynamic light scattering measurements (BI 200SM, Brookhaven Instruments, Holtsville, NY).

Hydrophilic Solute Transport

For the transport experiments using purified Cx43 and mutants, radiolabeled probes were loaded by extrusion during the production of liposomes or proteoliposomes (Bao *et al*., 2004b). After loading, the samples were run through a gel filtration column to remove the extraliposomal probe, and the radiolabel retained by the proteoliposomes was determined by liquid scintillation counting. The radiolabels used were ^{14}C-sucrose and ^{14}C-maltose (Amersham Biosciences, St. Louis, MO) and ^{14}C-ethyleneglycol (American Radiolabeled Chemicals, Piscataway, NJ). Background from probe trapped into compartments inaccessible for transport was assessed by permeabilization with 0.1% DMSO as described (Bevans *et al*., 1998).

LRET experiments

For the LRET experiments, purified connexins solubilized in 0.3% decylmaltoside were divided in three aliquots. One remained unlabeled and the others were labeled with either fluorescein maleimide (Invitrogen, Carlsbad, CA) or Tb^{3+}-DTPA-cs124-EMCH (DTPA, diethylenetriaminepentaacetate; EMCH,-maleimido caproic acid hydrazide), by incubation for 2 h at 4°C with a 10-fold molar excess of the thiol reagents. Details on the properties and synthesis (performed in the Organic Chemistry Core Laboratory at the University of Texas Medical Branch) of Tb^{3+}-DTPA-cs124-EMCH have been published (Chen and Selvin, 1999). DTPA-cs124-EMCH contains carbostyril 124 as an "antenna" that absorbs the incident light from a nitrogen laser source and transfers it to the Tb^{3+}, which by itself displays a weak absorbance. The chelator in DTPA-cs124-EMCH, binds the lanthanide tightly and shields it from the

quenching effects of water. The thiol-selective maleimide group from EMCH allows for protein labeling. After protein labeling, the unreacted compounds were removed by gel filtration, and unlabeled and labeled proteins were mixed in varying proportions and incubated for at least 2 h before the experiments. This time was sufficient for essentially complete subunit exchange between detergent-solubilized hemichannels (the subunit exchange halftime is 14 min, see **RESULTS**). In some experiments, the mixtures were reconstituted into liposomes for the LRET measurements. The samples were analyzed in 100-µl quartz cuvettes. Excitation at 337 nm was carried out with a 1.45-MW pulsed nitrogen laser (GL-3300; Photon Technology International, Birmingham, NJ; 1-ns pulses at 10 Hz). Luminescence spectra were recorded on a TM11 phosphorescence lifetime system (Photon Technology International) with an R928 photomultiplier detector (Hamamatsu, Bridgewater, NJ). For most measurements, the emission monochromator was removed and replaced by band-pass filters to increase light throughput. The bandpass filters for fluorescein (XB88, 520DF10) and Tb^{3+} detection (XB91, 540DF10) were from Omega Optical (Brattleboro, VT). Steady-state fluorescence was measured on a fluorolog-2 spectrofluorometer (SPEX Industries, Edison, NJ).

Statistics

Data are presented as means ± SEM, and statistically significant differences were assessed by the *Student t*-test for paired or unpaired data, or one-way ANOVA, as appropriate.

RESULTS

Characterization of hemichannels purified in decylmaltoside

To test the function of purified hemichannel preparation in decylmaltoside, I reconstituted dephosphorylated Cx43 (permeable to "large" hydrophilic solutes, see Bao *et al*., 2004b) in 100-nm-diameter unilamellar liposomes at average ratios of 0.8 or 2.3 hemichannels/liposome. Under these conditions, 60% and 90% of the liposomes containing dephosphorylated Cx43 are predicted from the Poisson distribution to be permeable to sucrose, respectively. The experimental values, measured using a rapid filtration assay (Bao *et al*., 2004b), were 66 ± 5 (n = 4) and 90 ± 5% (n = 7) for the 0.8 or 2.3 hemichannels/liposome average ratios, respectively. These data indicate that most, if not all, reconstituted hemichannels are functional, and that the fraction of purified Cx43 that can form functional hemichannels is higher than that observed when octylglucoside was the detergent (Bao *et al*., 2004b). The analysis of the oligomeric state of Cx43 and Cx43-EGFP showed that in decylmaltoside, at protein concentrations >1 mg/ml, essentially all Cx43 and Cx43-EGFP molecules form hexamers (see Fig. 3.6 for an example), whereas under similar conditions in octylglucoside, 20–25% of the protein remained as monomers (Bao *et al*., 2004b). Based on these observations and data by others (Kistler *et al*., 1994), I decided to use decylmaltoside as the detergent of choice for Cx43 solubilization and purification.

Comparison of the properties of purified hemichannels with those of hemichannels in cell plasma membranes

Our laboratory has previously shown that purified hemichannels, as prepared here, are functional (permeable to "large" hydrophilic solutes of up to 1,000 Da molecular weight) and blocked by PKC-mediated phosphorylation of Ser368 and millimolar extracellular [Ca^{2+}], similarly to hemichannels in cell plasma membranes (Bao *et al*., 2004a; Bao *et al*., 2004b; Bao *et al*., 2005). In Chapter 2, I showed extensive SCAM data on single Cx43 that lead to the identification of four M3 residues as pore-lining. These were identified primarily by the MBB block of the uptake of carboxyfluorescein elicited by lowering extracellular [Ca^{2+}] in frog oocytes. MBB is a cell-membrane impermeable thiol reagent that can access the hemichannel pore (see Chapter 2). Based on the results in Chapter 2 (Fig. 2.3 to 2.5), I selected the four mutants that displayed MBB sensitivity (I156C, F161C, V164C and V167C), as well as three that did not (I157C, S158C and K162C).

For the transport studies we measured retention of radiolabeled sucrose after gel filtration of proteoliposomes preloaded with radiolabeled probe as described in **METHODS**. For the transport studies, I took advantage of the observation that purified Cx43 hemichannels dephosphorylated by alkaline phosphatase are permeable to sucrose (phosphorylation by PKC abolishes sucrose permeability; Bao *et al*., 2004b). All the mutant hemichannels studied display sucrose permeability when the protein is dephosphorylated (the proteoliposomes do not retain sucrose), and the patterns of MBB sensitivity (Fig. 3.3) and protection by IAA against the MBB inhibition (Fig. 3.4) are identical to those in the same mutants expressed in the oocyte plasma membrane (compare to Fig. 2.3 and 2.4 in Chapter 2). These results, as those in Chapter 2, suggest a face of M3 that lines the Cx43 pore (Fig. 3.5). An interesting observation is that in the

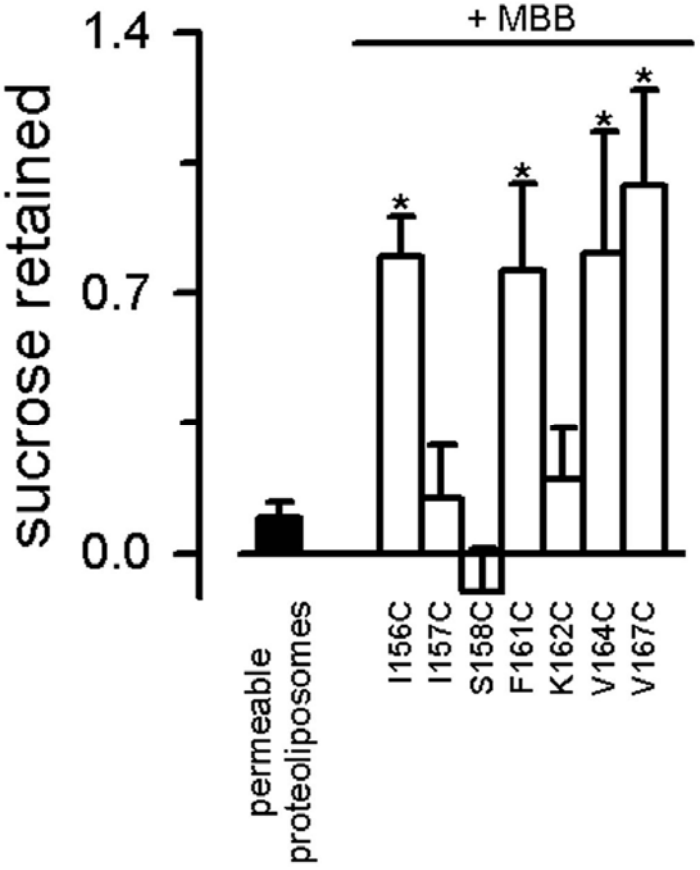

Figure 3.3: Effects of MBB (+ MBB) on sucrose efflux from proteoliposomes containing purified Cx43 hemichannels.

Radiolabeled sucrose was loaded into the proteoliposomes produced by the dialysis/extrusion method. Gel filtration was used to separate the free radioactive probe from the liposomes, and the fraction of sucrose retained inside the proteoliposomes was determined. The data were normalized to those in proteoliposomes containing sucrose-impermeable Cx43 hemichannels (PKC-phosphorylated Cx43) or liposomes without Cx43. The filled bar corresponds to DMSO-permeabilized liposomes. Data are means ± SEM from >3 independent experiments. * $P < 0.05$ compared to the value in the absence of MBB. These results show that the pattern of MBB sensitivity of M3 is the same in hemichannels expressed in the plasma membrane (see Fig. 2.3) and purified and reconstituted hemichannels.

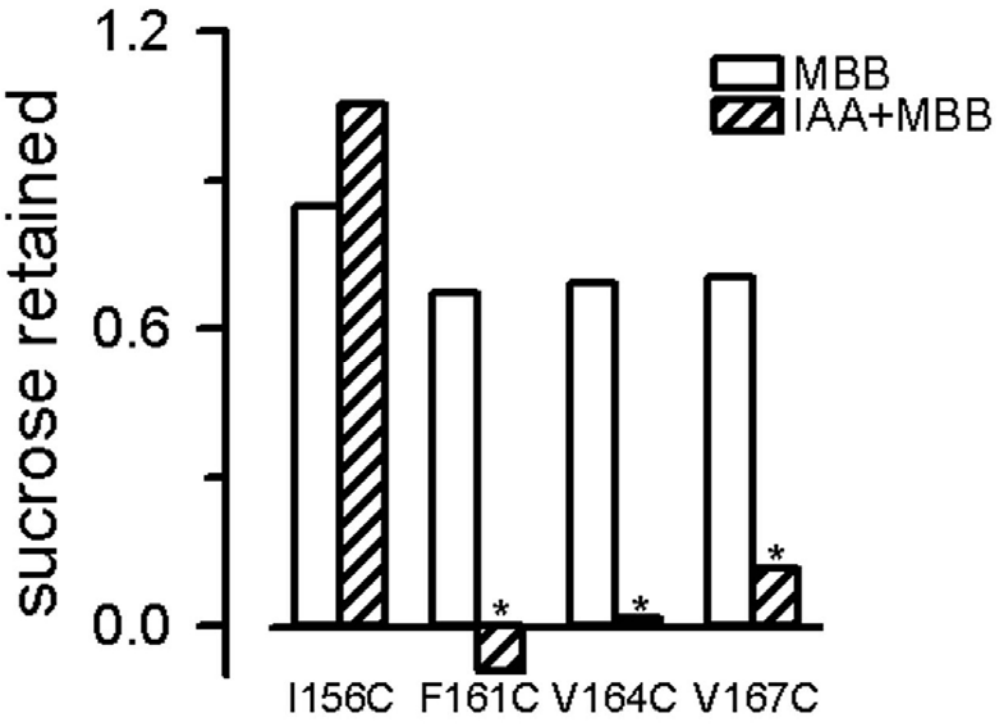

Figure 3.4: Protection of the inhibition by MBB of sucrose efflux by prior reaction with IAA.

When indicated, the proteoliposomes were exposed to 100 μM MBB for 10 min, before gel filtration. For the IAA experiments, the proteoliposomes were exposed to 10 mM IAA for 5 min, and then MBB was added as described above. Data are means ± SEM from 3 independent experiments. * $P < 0.05$ compared to the value in the absence of MBB. For experimental details and data normalization see Fig. 3.3. These results show that IAA protects from the block by MBB the same residue positions in hemichannels expressed in the plasma membrane (see Fig. 2.4) and hemichannels purified and reconstituted.

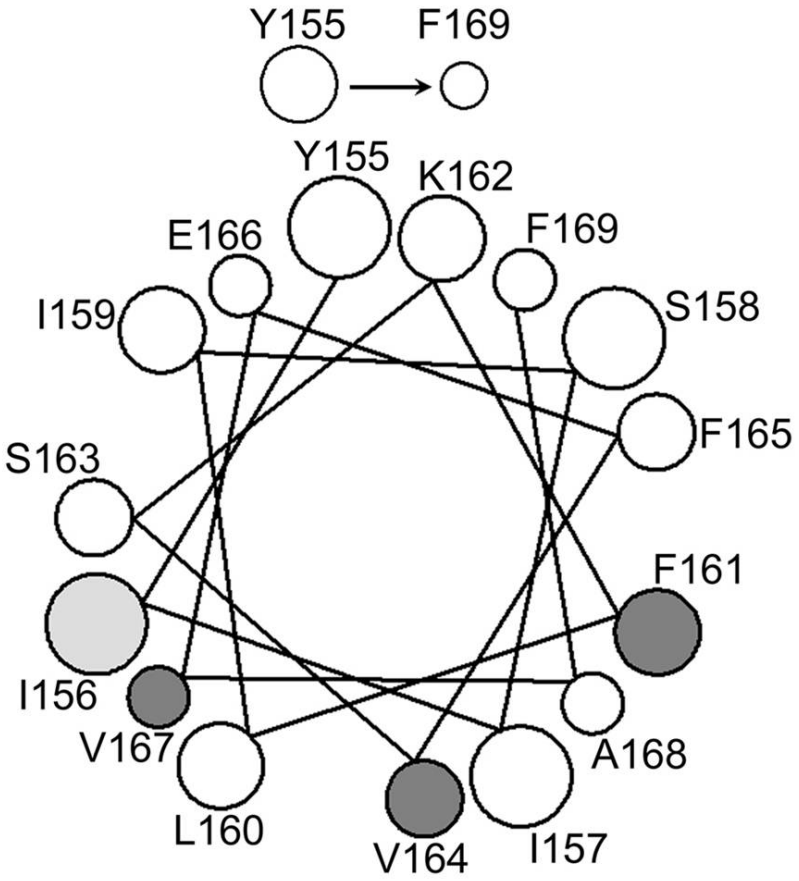

Figure 3.5: M3 helix-wheel summarizing the SCAM experiments. The residue positions sensitive to MBB are in gray (both lighter and darker gray). The positions where IAA prevented the effect of MBB are shown in dark gray. Note that all the MBB-sensitive lie on one helix face.

proteoliposomes containing single-Cys Cx43 mutants the reaction with the thiol probes is fast (complete in less than 5 min, see legend to Figs. 3.3 and 3.4). This suggests that the reactive Cys are readily accessible to the solvent.

Generation of purified hemichannels of controlled subunit composition

In previous studies from our laboratory (Bao *et al*., 2004b) and data shown in Fig. 3.6, we observed that at a concentration of 20 μM, solubilized Cx43-EGFP forms hexamers, as assessed by gel filtration. The first indication of a dynamic oligomerization process was suggested by additional gel filtration studies that showed that upon rerunning the Cx43-EGFP hexamers after sample dilution, Cx43-EGFP elutes as monomers (data not shown). To demonstrate subunit exchange, we studied decylmaltoside-solubilized hemichannels by gel filtration chromatography. To this end, we mixed Cx43 with Cx43-EGFP. The 26-kDa EGFP increases the molecular mass significantly, allowing for detection of mixed oligomers. Fig. 3.6 shows that mixing of hemichannels formed by Cx43 with those formed by Cx43-EGFP yields hemichannels containing both Cx43 and Cx43-EGFP. The quantitative molecular mass analysis of the major peaks is consistent with Cx43 hexamers (Fig. 3.6, black traces), Cx43-EGFP hexamers (Fig. 3.6, green traces), and "mixed" Cx43/Cx43-EGFP hexamers (Fig. 3.6, red traces). The detergent bound to the hexamers (assessed from the difference between the calculated molecular mass and that expected from six connexins) seems to be 5–10% of the hexamer weight. Clearly, the Cx43:Cx43-EGFP mix localizes mostly to a peak that elutes between the hexamers of Cx43 and Cx43-EGFP. The peak of the hexamer mix is only slightly wider than those of the Cx43 and Cx43-EGFP hexamers and does not extend from the Cx43-EGFP to the Cx43 peaks, indicating that it corresponds to mixed Cx43:Cx43-EGFP hemichannels and not to separate Cx43 and Cx43-EGFP that coexist without connexin

exchange. A more detailed characterization of the subunit composition of "mixed" hemichannels was performed by LRET and is shown in the next section.

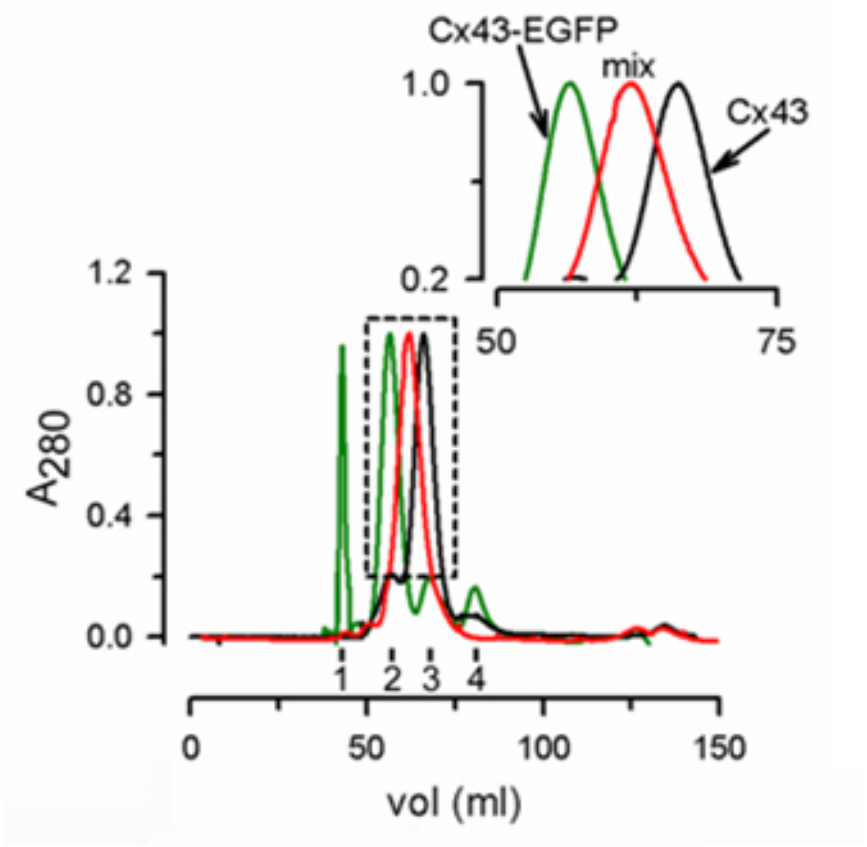

Figure 3.6: Gel-filtration chromatography of hemichannel mixtures.

Gel-filtration chromatography of hemichannel mixtures. Purified Cx43 and Cx43-EGFP gently mixed overnight at a 4:2 molar ratio, at 4°C, were analyzed by gel filtration in 0.3% decylmaltoside, 150 mM NaCl, 0.1 mM EDTA, and 10 mM Hepes/NaOH, pH 7.5. Ferritin (440 kDa, labeled 2) and aldolase (158 kDa, labeled 4) or thyroglobulin (669 kDa, labeled 1), catalase (232 kDa, labeled 3), and aldolase (158 kDa, labeled 4) were mixed with Cx43 and Cx43-EGFP, respectively, before injection into the FPLC system. Absorbance was measured at 280 nm (A280) and normalized to the hexamer peak values. From Bao *et al*. (2007). These data show that mixing of Cx43 and Cx43-EGFP hemichannels in detergent produces Cx43/Cx43-EGFP hemichannels.

Analysis of hemichannel subunit composition by LRET

To improve the analysis of mixed hemichannels, we developed a method based on LRET, using as donor the rare element Tb^{3+}, characterized by a long lifetime emission (Selvin, 2002) and, as acceptor, fluorescein. I measured LRET between Cx43 subunits labeled with either Tb^{3+} or fluorescein to determine the composition of hemichannels based on the number of acceptor-labeled monomers *per* hemichannel. LRET is sensitive and independent of the connexin molecular weight and has been used in a few studies of membrane proteins to assess inter-subunit and intramolecular distances (Cha *et al*., 1999; Vázquez-Ibar *et al*., 2002; Knauf and Pal, 2004; Posson *et al*, 2005; Pal *et al.*, 2005). LRET has many advantages for our experiments when compared with traditional FRET, which translate in very low background, high signal-to-noise ratio, and independence of the labeling stoichiometry (Selvin, 2002; Cha *et al*., 1999).

I mixed fluorescein-labeled, Tb^{3+}-labeled and unlabeled Cx43 in different proportions, with a low proportion of Tb^{3+}-labeled Cx43 (0.5 mol *per* hemichannel), to assure that most hemichannels had zero or one Tb^{3+}-labeled Cx43 subunit, and only a small percentage (8%; calculated from the binomial distribution) had more than one donor-label subunit. Under these conditions, and considering that essentially all subunits are assembled as functional hemichannels (see **RESULTS** above and Bao *et al*., 2004b), the amplitude of fluorescein emission caused by energy transfer from Tb^{3+} (sensitized fluorescein emission with long lifetime) depends on the number of acceptors (fluorescein-labeled Cx43 *per* hemichannel) and can be used to determine the subunit composition of the hemichannels. This is because all LRET under the conditions of my experiments occurs between subunits in a hemichannel. There is no intramolecular LRET because subunits are labeled with either donor or acceptor separately, before mixing. Because of the long distances involved (>1,000 Å) and the high dependence of energy

transfer on the distance (inversely proportional to the sixth power of the distance), LRET between hemichannels in solution or hemichannels in different liposomes is negligible. The absence of inter-hemichannel LRET was demonstrated by measuring the time course of the increase in sensitized emission upon mixing two populations of detergent-solubilized hemichannels, one labeled with Tb^{3+} and the other one labeled with fluorescein. From such experiments, a halftime of subunit exchange of 14 min was measured, with essentially no signal immediately after mixing (shown later). Also, there was no significant LRET when two sets of proteoliposomes, one containing donor-labeled hemichannels and another one containing acceptor-labeled hemichannels, were mixed (data not shown).

WT Cx43 contains nine Cys of which at least four are likely to form intramolecular disulfide bonds (Foote *et al*., 1998). Under the labeling conditions of most of my experiments, the stoichiometry of labeling was 3.2 ± 0.1 fluorescein molecules (n = 4) or 3.1 ± 0.1 Tb^{3+} (n = 3) *per* Cx43. These findings suggest that only 1/3 of the Cys in WT Cx43 are accessible to the labeling reagents.

In experiments with wild-type Cx43 hemichannels in which the labeling stoichiometry was reduced to 1 by reducing the labeling time, a decrease in the magnitude of the signal was observed, but the relationship between LRET and the number of fluorescein-labeled subunits was not affected (data not shown). Additional data showing independence of the methodology on the labeling stoichiometry and the absence of significant background (measured on Cys-less Cx43 hemichannels) are presented later in this section. Connexin labeling and the LRET data were also independent of whether Cx43 was dephosphorylated or PKC-phosphorylated (data not shown). Therefore, the assembly of detergent-solubilized Cx43 into hemichannels does

not depend on phosphorylation, confirming previous observations from our laboratory (Bao *et al*., 2004b).

Fig. 3.7A shows that, as expected, the steady-state fluorescence increases with the content of fluorescein-labeled Cx43 *per* hemichannel. The important result is that when the emission is measured in a gated mode (without recording during the first 60 μs after a 1-ns nitrogen laser pulse), the fluorescein emission caused by direct excitation is very low (Fig. 3.7B, black trace). This finding is expected from the short duration of the excitation pulse (1 ns) and the short lifetime of the fluorescein excited state (4–5 ns). In addition, the lack of signal from scattering of the excitation pulse and the sample autofluorescence, caused by the short excitation pulse and nanosecond lifetimes of native fluorophores, combine to contribute to a low emission background. Fig. 3.7B (blue trace) shows that lanthanide emission is in sharp peaks with interposed dark regions (Selvin, 2002), and therefore measuring at wavelengths where the donor does not emit eliminates the luminescence of the lanthanide complex itself. The red trace in Fig. 3.7B shows an emission with a peak at 520 nm that corresponds to sensitized emission from fluorescein, *i.e.*, emission resulting from LRET from Tb^{3+}, as opposed to direct fluorescein excitation. As mentioned above, the latter is essentially absent in the sample containing only fluorescein-labeled Cx43 (Fig. 3.7B, black trace). Therefore, the sensitized emission from fluorescein is easily isolated by using a bandpass emission filter (Fig. 3.8A), with negligible background fluorescence (Figs. 3.7B and 3.8A, black traces).

As expected for energy transfer, sensitized fluorescein emission increased (Fig. 3.8A) as a function of the number of acceptors *per* hemichannel. There was also shortening of the lifetime of the donor, which in LRET translates in the decreased sensitized emission, clearly apparent in Fig. 3.8B (see Inset for a direct comparison). Fig. 3.8C shows that the sensitized fluorescein emission is proportional to the number of

fluorescein-labeled Cx43 *per* hemichannel. Experiments with reconstituted hemichannels formed by a mutant Cx43 containing a single Cys at position 156 (I156C mutant, labeling stoichiometry of 0.9 ± 0.1, n = 4) showed the expected increase in LRET when the number of fluorescein-labeled subunits increased. In reconstituted hemichannels containing averages of two and four acceptor-labeled subunits, LRET values increased by 76 ± 12 and 145 ± 15%, respectively, compared with the average measured in

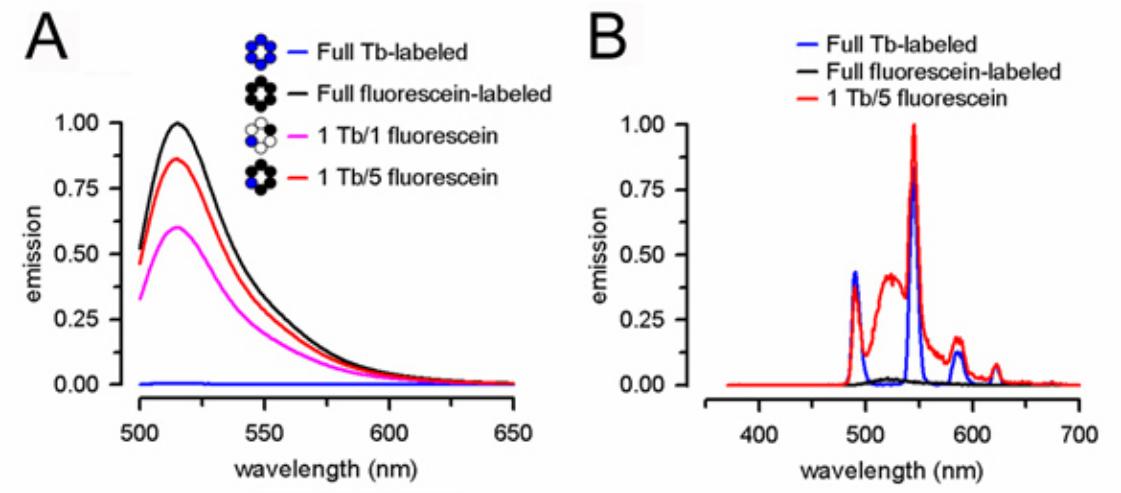

Figure 3.7: Luminescence resonance energy transfer between Tb^{3+}- and fluorescein-labeled Cx43 subunits in hemichannels.

Purified WT Cx43 solubilized in 0.3% decylmaltoside was labeled with either fluorescein maleimide or Tb^{3+}-DTPA-cs124-EMCH, by incubation for 2 h at 4°C with a 10-fold molar excess of the thiol reagents. Unreacted labels were removed by gel filtration and unlabeled and labeled proteins were mixed in varying proportions and incubated for at least 2 h before analysis. A. Steady-state fluorescence emission spectra (excitation at 490 nm). Data normalized to peak value of fully fluorescein-labeled preparation. B. Gated emission spectra (60-µs delay after a 337 nm 1-ns pulse from a nitrogen laser). Control experiments showed that at the concentrations present during Cx43 labeling, there is no significant LRET between free Tb^{3+} and free fluorescein after gel filtration. Data were normalized to the peak value of 1 Tb/5 fluorescein-labeled preparation. Traces are representative from four independent experiments. From Bao *et al*. (2007).

hemichannels containing 1 acceptor-labeled subunit (n = 4, P < 0.001). The corresponding values for similar experiments using WT Cx43 hemichannels (labeling stoichiometry of 3) yielded increases in LRET of 49 ±11 and 125 ± 16%, respectively (n = 7, P < 0.001). These results support the contention that the relationship between LRET and the number of acceptor subunits is maintained at varying subunit labeling stoichiometries.

As a control, I also performed experiments in proteoliposomes containing hemichannels formed by Cys-less Cx43, to determine whether potential impurities in the

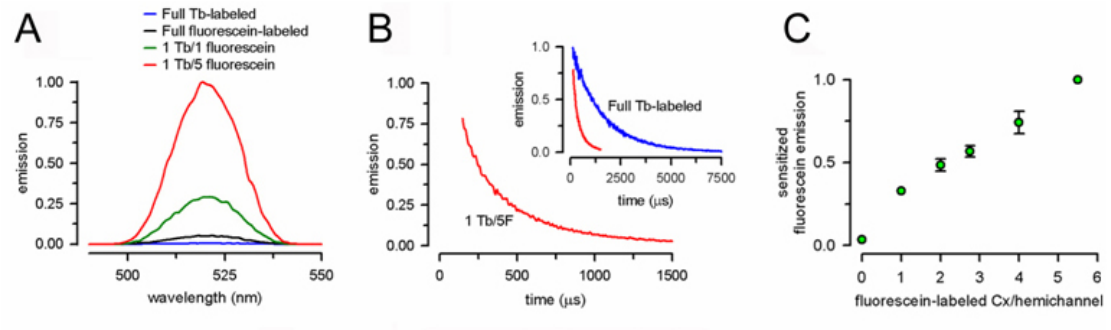

Figure 3.8: Determination of hemichannel composition from LRET data

A. Sensitized fluorescence emission (60-µs delay after pulse), normalized as described in Fig. 3.7B. B. Time course of sensitized fluorescence emission (520 ± 20 nm bandpass filter, red). (Inset) Donor Tb^{3+} emission (540 ± 20 nm filter, blue trace) and sensitized emission (red trace) lifetimes. Data in A and B correspond to typical traces that were obtained by using Cx43 solubilized in decylmaltoside at a concentration >1.5 mg/ml. C. Sensitized fluorescence emission as a function of the average number of fluorescein-labeled connexins *per* hemichannel. Data were normalized to the peak value of 1 Tb/5.5 fluorescein-labeled preparation and are presented as means ± SEM of seven to nine experiments. Cx43 hemichannels were reconstituted at a ratio of 0.8 hemichannels *per* liposome (20 µg protein *per* measurement). Similar results were obtained in detergent-solubilized Cx43 at >1.5 mg/ml (data not shown), where essentially all Cx43 subunits form hemichannels (see Fig. 3.6). All values are statistically different from the previous one (P < 0.001), except for that at the 3/3 ratio. For additional details see Fig. 3.7. From Bao *et al*. (2007).

preparation that are not detected by standard biochemical techniques, or other unforeseen factors, contribute to LRET. LRET measured in reconstituted hemichannels containing CL Cx43 subunits reacted with the Tb^{3+} or fluorescein thiol reagents, mixed to obtain

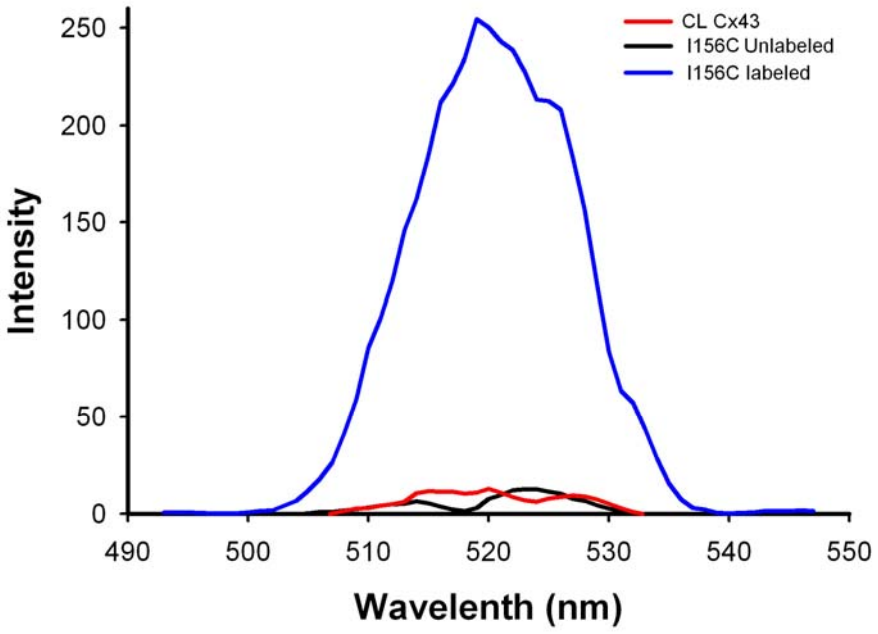

Figure 3.9: Comparison of sensitized-fluorescein emission from hemichannels formed by unlabeled single-Cys I156C mutant, the same mutant labeled with Tb^{3+} and fluorescein, and labeled Cys-less hemichannels.

Sensitized fluorescein emission was recorded after a 60-μs delay after pulse. The subunits were mixed to obtain one subunit labeled with donor and one subunit labeled by acceptor *per* hemichannel. These data show the high signal-to-noise ratio of the LRET emission in single-Cys mutants hemichannels under the same conditions, a value not different from the background measured in hemichannels containing unlabeled subunits (3 ± 3%, n = 9).

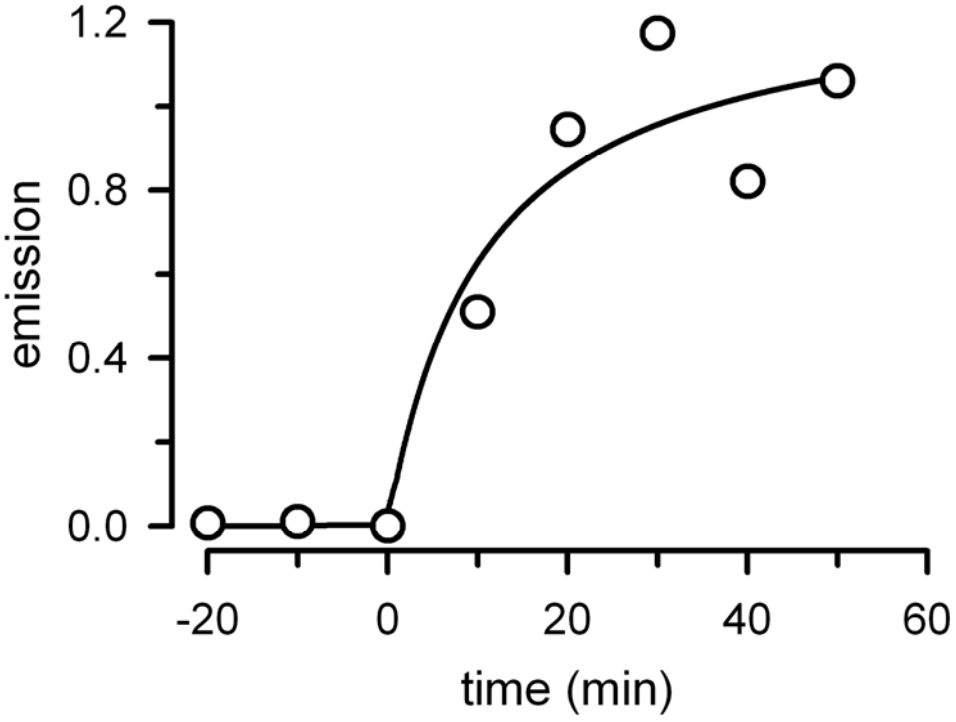

Figure 3.10: Time course of the exchange between hemichannel subunits solubilized in decylmaltoside

Sensitized fluorescence emission (160-μs delay after pulse) was normalized to the maximal emission (emax) calculated from a hyperbolic fit to the data: $e = e\max \times t/(e\max/2 \times t)$, where e is the emission intensity and t is time. The connexin concentration was ~1.5 mg/ml, sufficient to direct the assembly of hemichannels in detergent (see Fig. 3.6). Two preparations of purified and solubilized hemichannels were mixed at time = 0. One was labeled with donor only and the other one only with acceptor (average of 3 subunits labeled in each preparation). From this and similar data, a subunit exchange half-time (time for $e = e\max/2$) between 7 and 14 min was calculated. The result demonstrates exchange between hemichannel subunits in detergent.

hemichannels containing one subunit reacted with donor and another one with acceptor, gave LRET values that were only 9 ± 2% (n = 8) of those measured on CL Cx43-I156C

As mentioned under **RESULTS**, I performed some experiments to assess the time course of the increase in sensitized emission upon mixing two populations of detergent-

solubilized hemichannels, one labeled with Tb^{3+} and the other one labeled with fluorescein. Fig. 3.10 shows one such experiment, where essentially no signal was apparent immediately after mixing, and a progressive increase in sensitized emission followed. This increase is a consequence of the exchange of hemichannel subunits in detergent. At time = 0 there are two hemichannel populations, donor-labeled and acceptor-labeled, and there is no sensitized emission because the distance between the hemichannels is too long, *i.e.*, there is no inter-hemichannel LRET. As time progresses, the subunits exchange, forming hemichannels with donor-labeled and acceptor-labeled subunits, with the resulting increase in sensitized emission.

DISCUSSION

Because the generation of hemichannels of controlled composition was attempted *in vitro*, it was critical to demonstrate that there is exchange between solubilized Cx43 subunits and that the composition of the reconstituted hemichannels is that expected from the mixture ratio. Previous studies (Kistler *et al*., 2004; Cascio *et al*., 1995; Stauffer *et al*., 1991; Stauffer, 1995) have shown solubilization of gap-junctional plaques into hemichannels, but compared with our studies there were differences in the solubilization conditions and/or isoforms studied. Also, previous studies focus on solubilized hemichannels using electron microscopy, and the presence of monomers was not assessed (Kistler *et al*., 1994; Cascio *et al*., 1995; Stauffer *et al*., 1991; Stauffer, 1995). One possibility to explain the apparent discrepancies is the observation that the outcome of the solubilization depends on the nature of the membranes (Ahmad *et al*., 1999). When Cx32 synthesized *in vitro* in the presence of microsomes was solubilized with dodecylmaltoside, it appeared mostly as monomers, whereas supplementation with Golgi membranes increased the amount of solubilized hexamers significantly (Ahmad *et al*.,

1999). This effect was not observed for Cx26 (Ahmad *et al*., 1999), indicating that it is isoform-dependent. Insect cells have membranes of unusual properties and composition (Marheineke *et al*., 1998), which may explain why solubilization of Cx43 with several detergents yields monomers (at low concentrations), which can assemble as hexamers (at higher concentrations) that display subunit exchange. In the present study, we specifically looked at the possibility of exchange of subunits in solubilized hemichannels. Definitive evidence that exchange occurs was obtained from gel-filtration, LRET and sucrose-transport studies. The latter are shown in Chapter 5. It is important to mention that this subunit exchange occurs when the subunits are solubilized, and that we do not have evidence for exchange once the purified hemichannels are reconstituted.

One potential concern is that the purified hemichannels generated from solubilized subunits differ significantly from native hemichannels in cell membranes. This concern cannot be ruled out, but we have evidence for significant functional and structural similarities between native and purified hemichannels: 1) The permeability properties of native and purified Cx43 hemichannels are internally consistent, and phosphorylation of Ser-368 by PKC abolishes large-solute permeability in both purified and native hemichannels (Bao *et al*., 2004a; Bao *et al*., 2004b; Bao *et al*., 2004c; Bao *et al*., 2005; Bao *et al*., 2007). 2) The face of transmembrane helix 3 that lines the pore is the same in native and purified hemichannels, as determined by the substituted-Cys accessibility method. 3) The distances between homologous residues of transmembrane helices in diametrically opposed subunits are entirely consistent with the structure of Cx43 gap-junctional channels (see Chapter 4). In summary, the similarities between purified Cx43 hemichannels and hemichannels in the membrane of frog oocytes (MBB M3 residue accessibility patterns; permeability regulation by $[Ca^{2+}]$ and PKC) strongly suggest that the structure and function of native and purified hemichannels are similar.

LRET is sensitive and independent on the connexin molecular weight, and has been used in a few studies of membrane proteins to assess inter-subunit and intramolecular distances (Cha *et al.*, 1998; Knauf *et al.*, 2004; Posson *et al.,* 2005). In a given hemichannel containing a donor-labeled subunit, there will be energy transfer between each of the donors in the subunit and each of the acceptors in an acceptor-labeled subunit. Therefore, there will be nine energy-transfer processes between the donor subunit and each acceptor-labeled subunit. For the analysis of hemichannel subunit composition I use total energy-transfer data, without deconvoluting the individual transfers (which depend on the distances between each donor-acceptor pair, used for Chapters 4 and 5 calculations). Thus, each labeled subunit in a hemichannel can be treated as a donor or acceptor, with the sensitized emission between a donor-labeled and an acceptor-labeled subunit as the sum of the energy transfer arising from the nine donor–acceptor pairs. Because the energy transfer depends on the sixth power of the distance between donor and acceptor, the largest fraction of the total sensitized emission is the result of energy transfer between the Tb^{3+}-labeled subunit and the closest fluorescein-labeled subunits. However, considering a Förster distance (R_0, the distance at which the energy transfer efficiency is 50%) for the Tb^{3+}-fluorescein pair of 45 Å, and distances between subunits in a hemichannel <100 Å, even the acceptor-labeled subunit diametrically opposed to the donor-labeled subunit contributes significantly to the total energy transfer in a hemichannel. In summary, all acceptor-labeled subunits contribute to the sensitized emission, and therefore the signal is proportional to the number of labeled subunits in the hemichannel.

The LRET-based method has several advantages compared with gel filtration for the determination of the composition of purified hemichannels. First, it is more accurate because it allows for discrimination between hemichannels containing ± 1 acceptor-

labeled subunits (only the difference between hemichannels with two vs. three acceptor-labeled subunits was not statistically significant). This discrimination is clearly superior to that achievable with gel filtration. Second, the measurements can be carried out easily in either proteoliposomes or solution. This is very important in the case of membrane proteins because it allows for parallel determinations of oligomerization and function.

The assessment of hemichannel composition using LRET and the ability to generate hemichannels of controlled subunit composition should be useful for studying disease-causing connexin mutants and assessing the effects of the isoform composition of hemichannels (heteromeric hemichannels) on permeability properties. One of the major advantages of LRET is that it can be used not only with proteins in solution, but also with lipid-reconstituted proteins. This property of LRET is essential for structural-functional studies of membrane proteins. Examples of the use of LRET to address specific issues will be presented in the next two chapters.